

Supporting Information
Hollow Mesoporous Carbon Nanocages
with Fe Isolated-Single-Atomic-Site derived
from MOF/polymer for High-Efficiency
Electrocatalytic Oxygen Reduction

*Congcong Wang, Yixin Chen, Ying Liu, Siyang Feng, Nan Zhang, Lin Shen, Kai Zhang**
and Bai Yang

State Key Laboratory of Supramolecular Structure and Materials, College of
Chemistry, Jilin University, Qianjin Street 2699, Changchun 130012, People's Republic
of China

*Address correspondence to zk@jlu.edu.cn

Material and methods

Materials and reagents.

2-Methylimidazole (99%, Aladdin), zinc nitrate hexahydrate ($\text{Zn}(\text{NO}_3)_2 \cdot 6\text{H}_2\text{O}$, Aladdin), iron acetylacetonate (99%, Aldrich) ($\text{Fe}(\text{acac})_3$, 99%, Aldrich), pyrrole (Py, 99%, Aladdin), Nafion® perfluorinated resin solution (5 wt.% in lower aliphatic alcohols and water, contains 15~20% water, Aldrich), commercial Pt/C (20 wt% metal), methanol (MeOH, HPLC), KOH (analytical grade, Beijing Chemical), N,N-dimethylformamide (DMF, analytical grade, Sinopharm Chemical) All of the chemicals used in this experiment were used as received without any further purification.

Synthesis of ZIF-8

1190 mg (4 mmol) $\text{Zn}(\text{NO}_3)_2 \cdot 6\text{H}_2\text{O}$ was dissolved in a mixture of 15 mL methanol and DMF ($V_{\text{MeOH}}: V_{\text{DMF}}=4:1$) to form a colorless and transparent solution. Then, 2628 mg (32 mmol) 2-Methylimidazole was dissolved into a mixture of 10 mL methanol and DMF ($V_{\text{MeOH}}: V_{\text{DMF}}=4:1$) to form a colorless and transparent solution. Finally, the above solution was evenly mixed and stood for 2 h. The product was centrifuged at 10000 rpm for 10 min, and then washed with methanol for three times. Finally, the white precipitation of ZIF-8 was dispersed in 40 mL methanol for standby use.

Synthesis of ZIF-8/Fe@PPy

6.7 mL of the above prepared ZIF-8 nanostructure was dispersed in 120 mL methanol, and 2 mL 5 mg/mL $\text{Fe}(\text{acac})_3$ methanol solution was added to mix evenly. Finally, 8 mL Py monomer was added and refluxed at 60 °C for 7 h to synthesize ZIF-8/Fe@PPy, and the solution changed from yellow to brown color gradually. After centrifugation (8000 rpm, 8 min) and washing with methanol for three times, the obtained precipitation was placed in a vacuum oven at 60°C and dried overnight to obtain the brown ZIF-8/Fe@PPy powder.

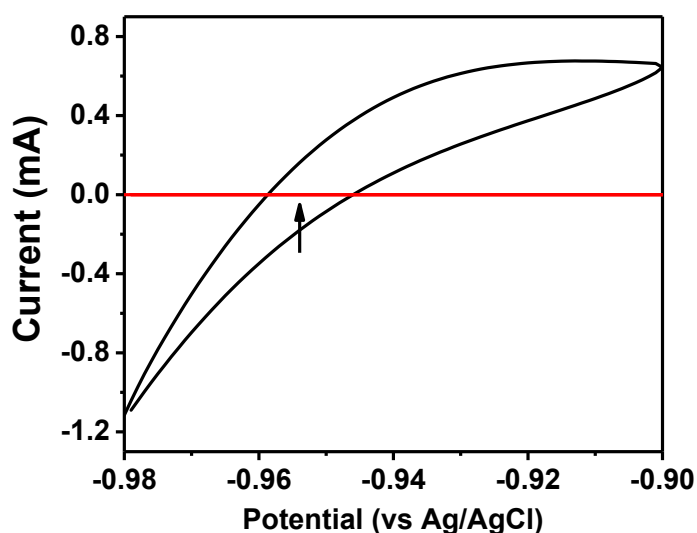
Synthesis of Fe-ISAs/H-CN

ZIF-8/Fe@PPy powder was calcined at 900 °C (heating rate 5 °C/min) for 3 h under the condition of argon protection and cooled naturally to room temperature without further treatment, resulting the black powder(Fe-ISAs/H-CN).

Electrochemical Measurement

All the electrochemical measurements were carried out in a conventional three-

electrode system on a CHI 760 electrochemical station (Shanghai Chenhua, China). A rotating disk electrode (RDE) with a glassy carbon (GC) disk of 5 mm in diameter was used as the substrate for the working electrode. Ag/AgCl ((saturated KCl solution) and a platinum wire were used as reference and counter electrode, respectively. The saturated electrode was used as the reference electrode in all measurements. It was calibrated with respect to reversible hydrogen electrode (RHE). The calibration was performed in the high purity hydrogen saturated 0.1 M KOH solution with 2×2cm platinum sheet as the working electrode. CV curves were run at a scan rate of 2 mv s⁻¹, and the average of the two potentials at which the current crossed zero was taken to be the thermodynamic potential for the hydrogen electrode reactions. The CV curves of RHE calibration was shown in below.



So in 0.1M KOH, $E(\text{RHE}) = E(\text{Ag}/\text{AgCl}) + 0.952 \text{ V}$

5 mg of catalyst was dispersed in 1 mL of solution containing 470 μL of ethanol and 470 μL of water and 60 μL of 5 wt.% Nafion solution and then sonicated for 1h to form a homogeneous catalyst ink. Then a certain volume of the catalyst ink was pipetted onto the GC surface with the Fe-ISAs/H-CN catalyst loading was 0.637 mg cm⁻² and the loading of Pt/C was 0.127 mg cm⁻². Before tests, O₂ flow was carried out through the electrolyte in the cell for about 30 min to achieve the O₂-saturated solution. The cyclic voltammetry (CV) tests were measured in O₂-saturated 0.1 M KOH solution with a scan rate of 50 mV s⁻¹. RDE tests were conducted in O₂-saturated 0.1 M KOH at different rotation rates with a sweep rate of 10 mV s⁻¹ at room temperature.

The electron transfer number (n) were determined by the Koutecky-Levich

equation:

$$J^{-1} = J_m^{-1} + J_k^{-1} = B^{-1} \cdot \omega^{-1/2} + J_k^{-1}$$

$$B = 0.62nF \cdot C_0 \cdot D_0^{2/3} \cdot \nu^{-1/6}$$

where J is the measured current density, J_k and J_L are the kinetic and limiting current densities, ω is the angular velocity of the disk, n is the overall number of electrons transferred in oxygen reduction, F is the Faraday constant (96485 C mol⁻¹), C_0 is the bulk concentration of O₂ (1.2 × 10⁻⁶ mol cm⁻³), D_0 is the diffusion coefficient of O₂ in 0.1 M KOH (1.9 × 10⁻⁵ cm² s⁻¹), and ν is the kinematic viscosity of the electrolyte (0.01 cm² s⁻¹), and k is the electron transfer rate constant.

2.6 Characterization

Transmission electron microscopy (TEM) images were collected on a Hitachi H-800 electron microscope operated at 200 kV with a CCD camera. High-resolution TEM (HRTEM) images and the energy dispersive spectrum (EDS) elemental mapping images were recorded using a JEM-2100F electron microscope at an acceleration voltage of 200 kV with a CCD camera. Aberration corrected high angle annular dark field-scanning transmission electron microscope (AC HAADF-STEM) images were taken on a JEM-ARM300F TEM/STEM with a spherical aberration corrector working at 300 kV. The X-ray absorption fine structure (XAFS) spectra data were collected at 1W1B station in Beijing Synchrotron Radiation Facility (BSRF), China. Scanning electron microscopy (SEM) images were taken with a JEOL FESEM 6700F electron microscope with an acceleration voltage of 3 kV. (The samples were sputtered with a thin layer of Pt prior to imaging). Inductively Coupled Plasma (ICP) results were conducted by OPTIMA 3300DV spectrometer. Fourier transform infrared (FTIR) spectra were taken on a Nicolet AVATAR 360 FTIR spectrophotometer. Nickel-filtered Cu $K\alpha$ radiation was used to perform X-ray diffraction (XRD) analysis, and the data were collected from 10 to 80° (model Rigaku RU-200B). An ESCALAB 250 spectrometer was used to perform X-ray photoelectron spectroscopic (XPS) analysis. The pore-size distribution was calculated via the Barrett–Joyner–Halenda (BJH) method, and the specific surface area was calculated via using the BJH and Brunauer – Emmett–Teller (BET) methods.

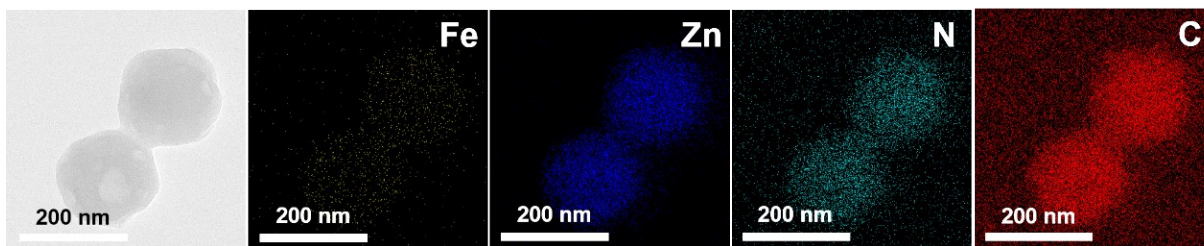


Fig.S1 The corresponding element maps of the ZIF-8/Fe@PPy. (Fe: yellow, Zn: blue, N: cyan, C: red)

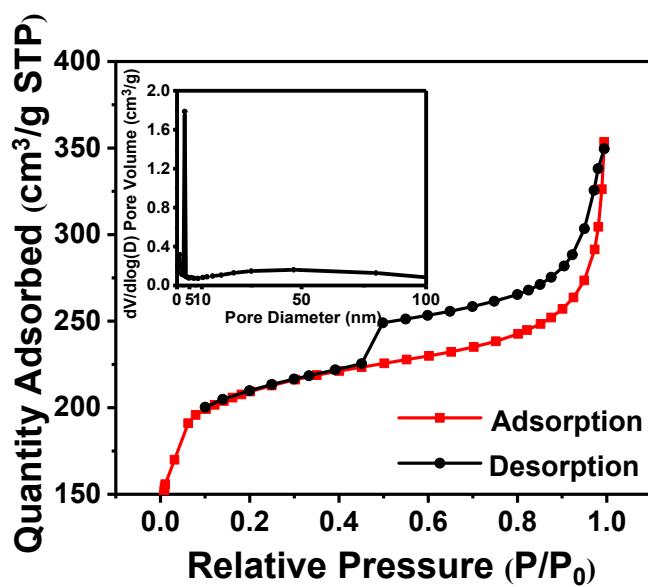


Fig.S2 Nitrogen adsorption/desorption isotherm of the ZIF-8/Fe@PPy catalyst. Top inset: corresponding pore size distribution.

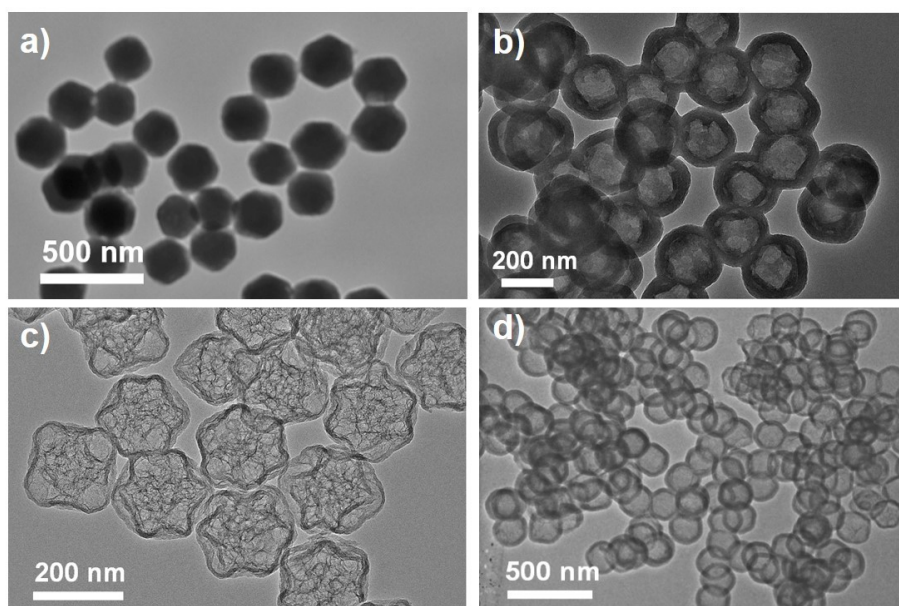


Fig. S3 TEM images of ZIF-8/Fe@PPy and Fe-ISAs/H-CN samples with different Py amount. a) 5 mL, b) 20 mL of ZIF-8/Fe@PPy; c) 5 mL, d) 20 mL of Fe-ISAs/H-CN.

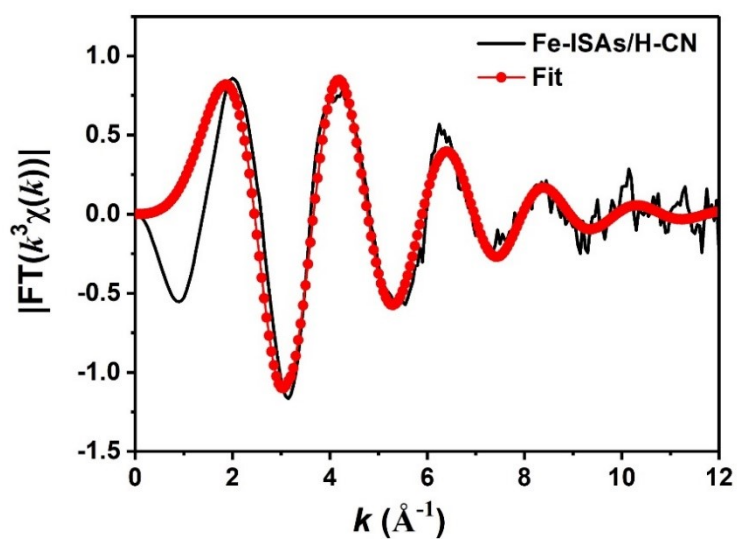


Fig. S4 The corresponding EXAFS k space fitting curves of Fe-ISAs/H-CN.

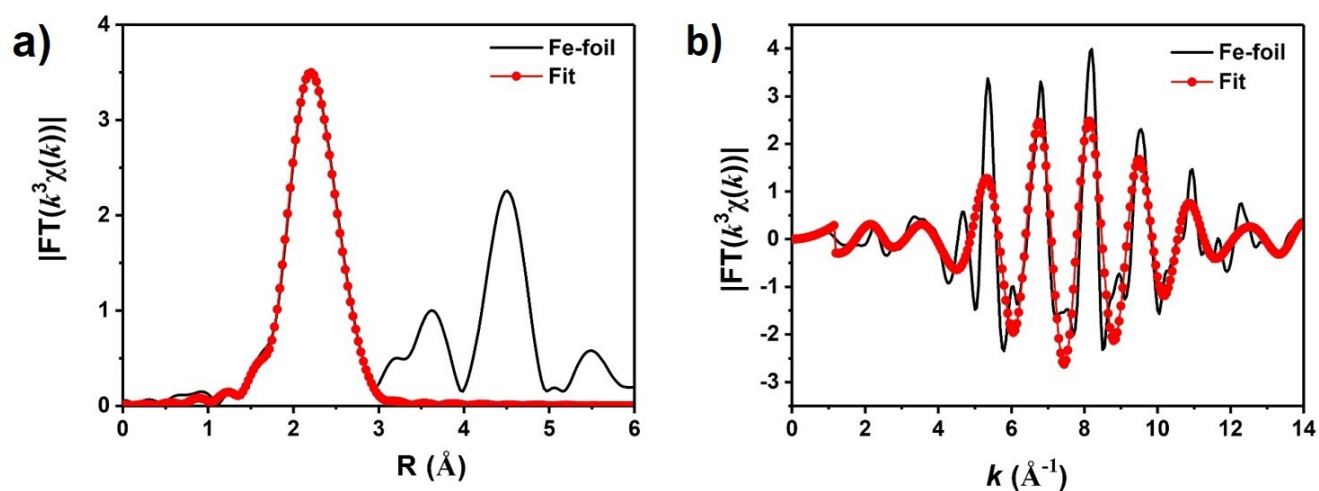


Fig. S5 EXAFS fitting curves of Fe foil. a) EXAFS R space fitting curves of the first shell Fe-Fe shell and b) EXAFS k space signal of the first Fe-Fe shell of Fe foil.

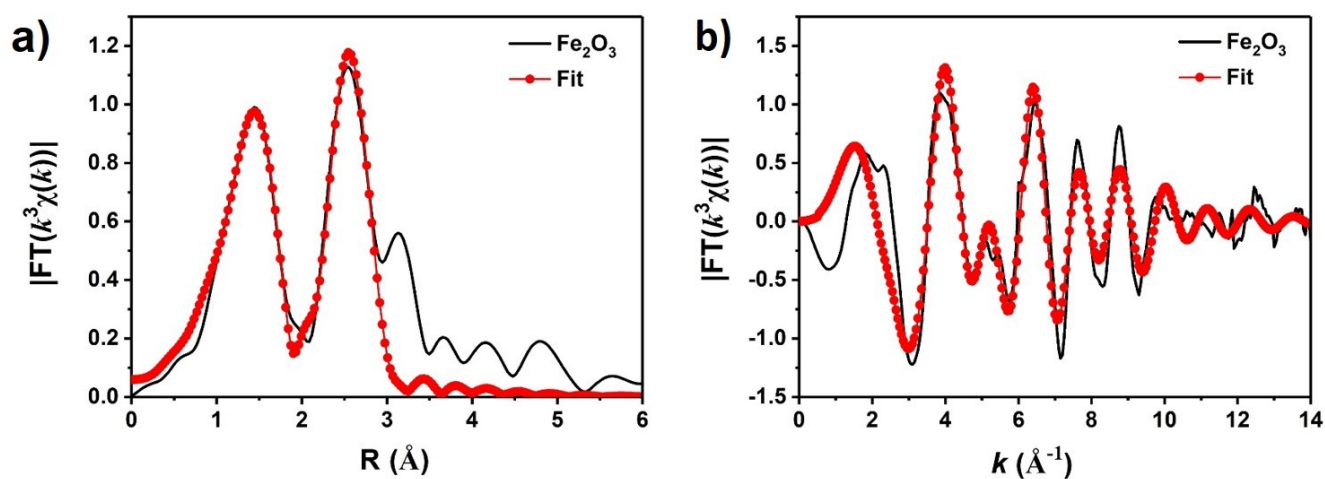


Fig. S6 EXAFS fitting curves of Fe₂O₃. a) EXAFS R space fitting curves for the Fe-O shell and b) EXAFS k space signal from the first Fe-O shell of Fe₂O₃.

Table S1 Fe K-edge EXAFS curves Fitting Parameters. ^[a]

	Path	N	ΔE (eV)	R(\AA)	$\sigma^2/10^{-3}(\text{\AA}^2)$	R-factor
Fe foil ^[b]	Fe-Fe1	8	5.06	2.46	4.15	0.006
	Fe-Fe2	6	5.06	2.85	4.15	
Fe ₂ O ₃ ^[c]	Fe-O	6	7.41	1.96	10.9	0.004
	Fe-Fe	6	5.96	2.99	8.85	
Fe-ISAs/H-CN	Fe-N	4.10	-1.40	1.99	12.0	0.004

[a] N, coordination number; R, distance between absorber and backscatter atoms; σ^2 , Debye–Waller factor to account for both thermal and structural disorders; ΔE , inner potential correction; R factor indicates the goodness of the fit. [b] Fitting range: $3.0 \leq k$ (\AA) ≤ 12.4 and $1.0 \leq R$ (\AA) ≤ 3.0 . [c] Fitting range: $3.0 \leq k$ (\AA) ≤ 11.5 and $1.0 \leq R$ (\AA) ≤ 3.0 . [d] Fitting range: $3.0 \leq k$ (\AA) ≤ 11.1 and $1.0 \leq R$ (\AA) ≤ 2.4 .

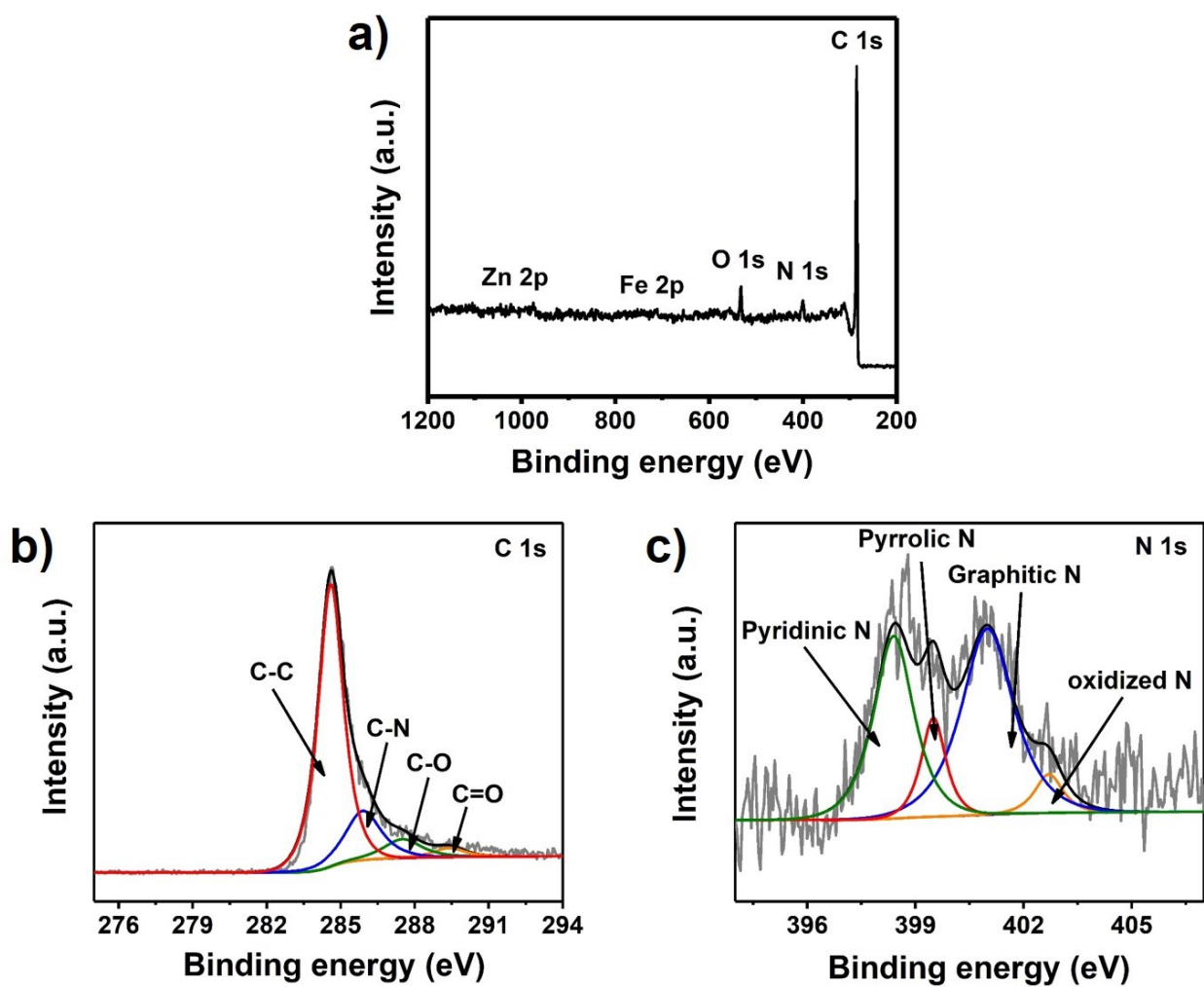


Fig. S7 The structure characterization of Fe-ISAs/H-CN catalysts. The high-resolution XPS spectra of a) XPS survey spectrum, b) C 1s, c) N 1s of the Fe-ISAs/H-CN catalysts.

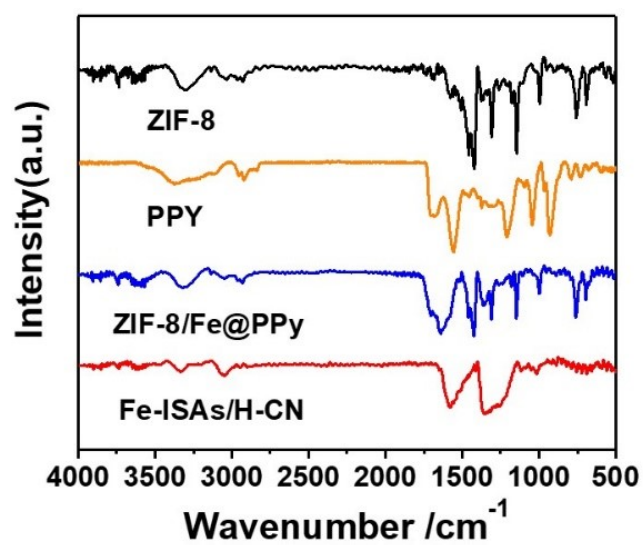


Fig. S8 FT-IR spectra of ZIF-8, PPy, ZIF-8/Fe@PPy and Fe-ISAs/H-CN.

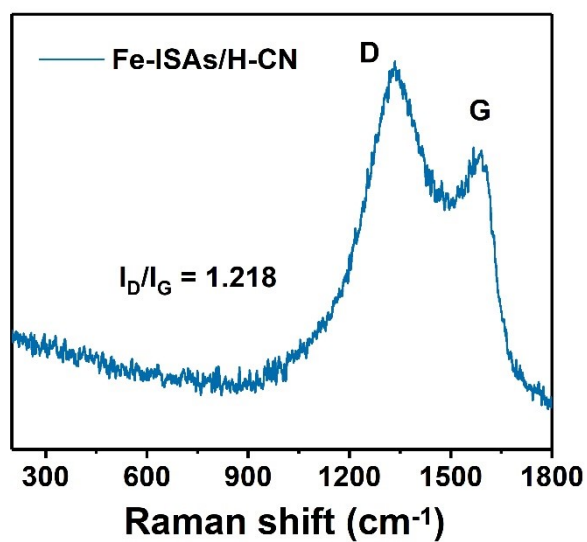


Fig. S9 Raman spectra for Fe-ISAs/H-CN under 900°C 3h.

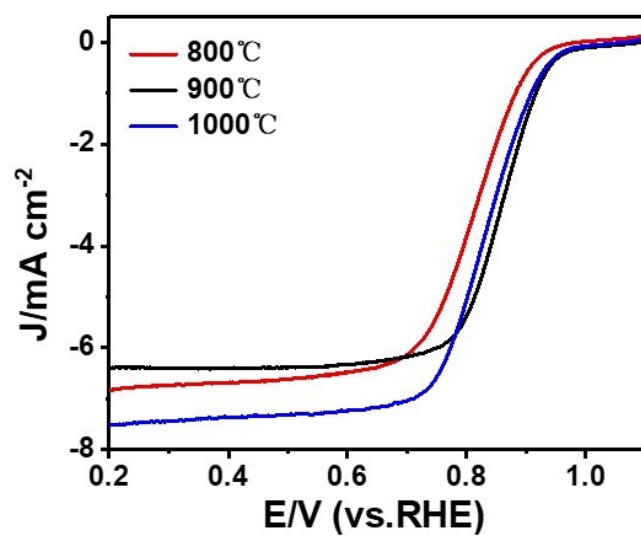


Fig. S10 Electrocatalytic oxygen reduction reaction performance for Fe-ISAs/H-CN under different temperature.

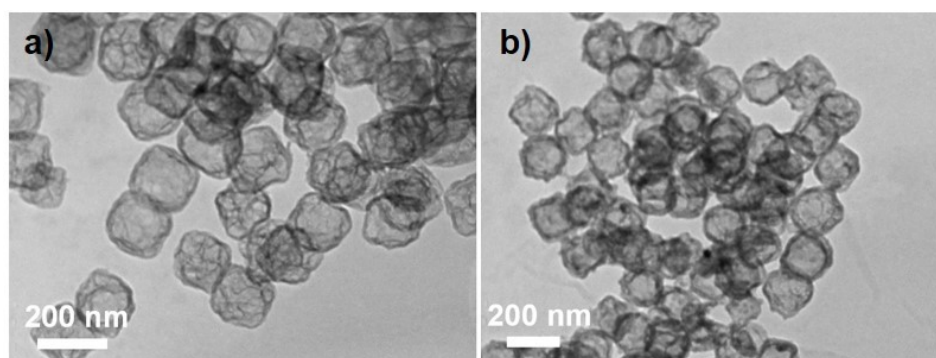


Fig. S11 TEM images of Fe-ISAs/H-CN under different temperature. a) 800°C, b) 1000°C.

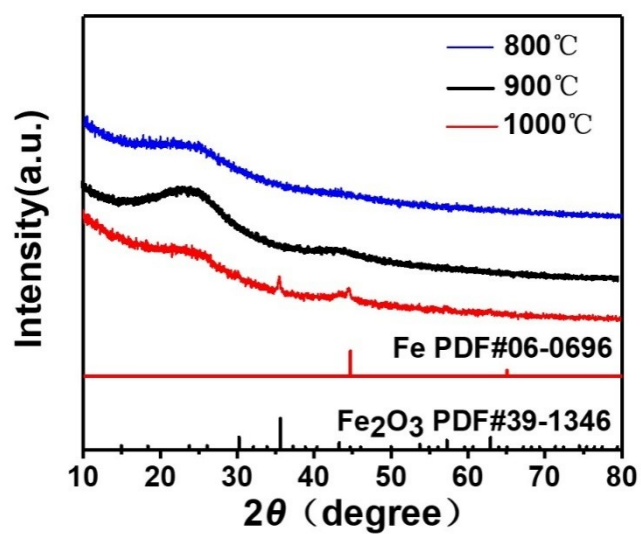


Fig. S12 XRD patterns of the Fe-ISAs/H-CN.

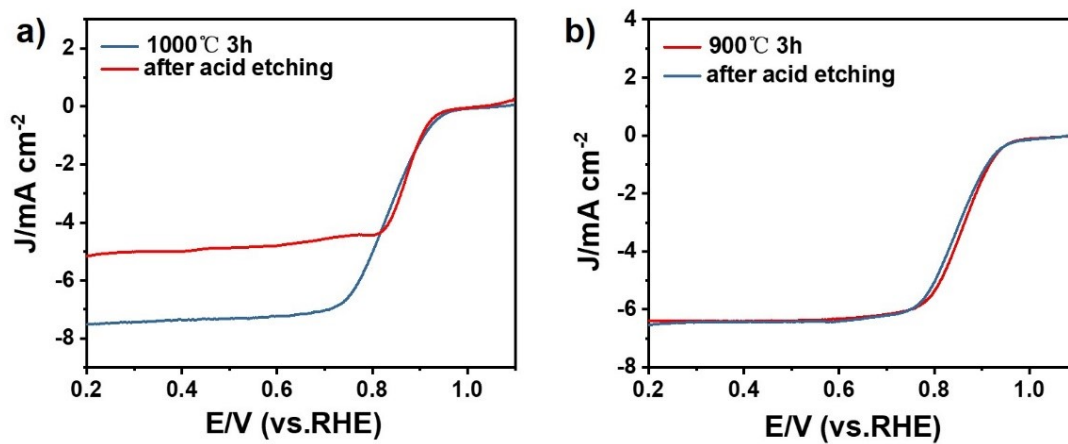


Fig. S13 Electrocatalytic oxygen reduction reaction performance for Fe-ISAs/H-CN a) under 1000 °C 3h and after acid etching; b) under 900 °C 3h and after acid etching

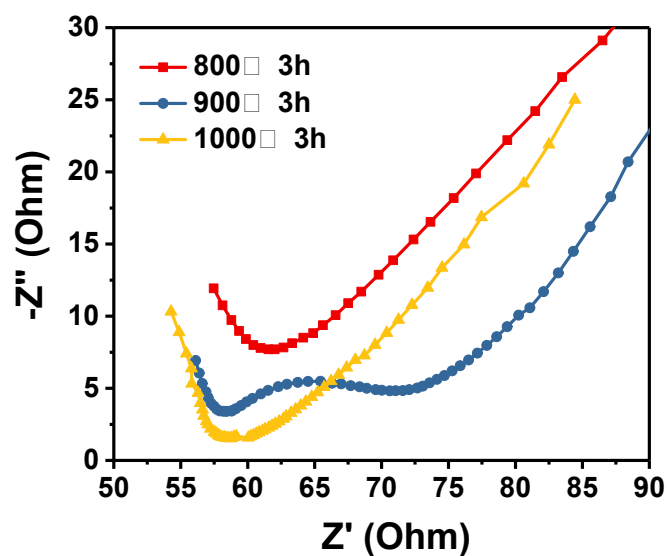


Fig. S14 Nyquist plots of electrochemical impedance spectroscopy (EIS) over Fe-ISAs/H-CN catalysts under different temperature in 0.1M KOH.

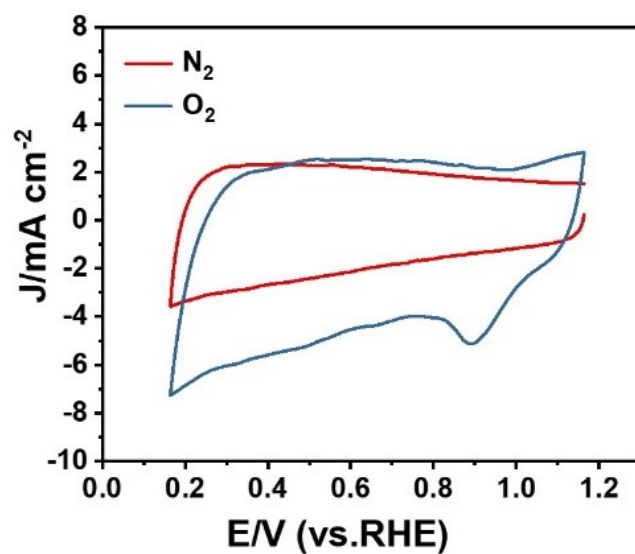


Fig. S15 CV curves of Fe-ISAs/H-CN in N_2 - and O_2 -saturated 0.1M KOH, respectively.

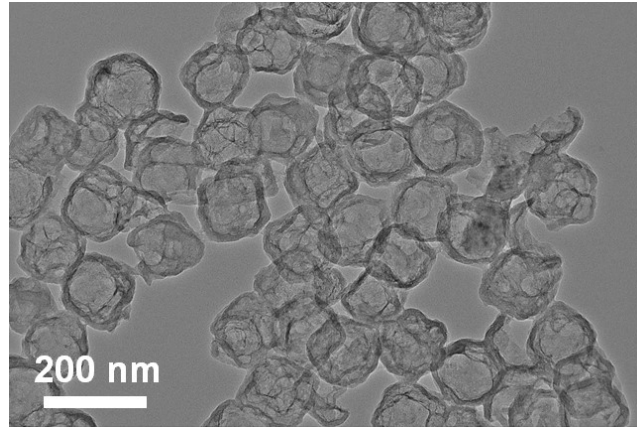


Fig. S16 TEM image of the Fe-ISAs/H-CN after the 10000 cycles.

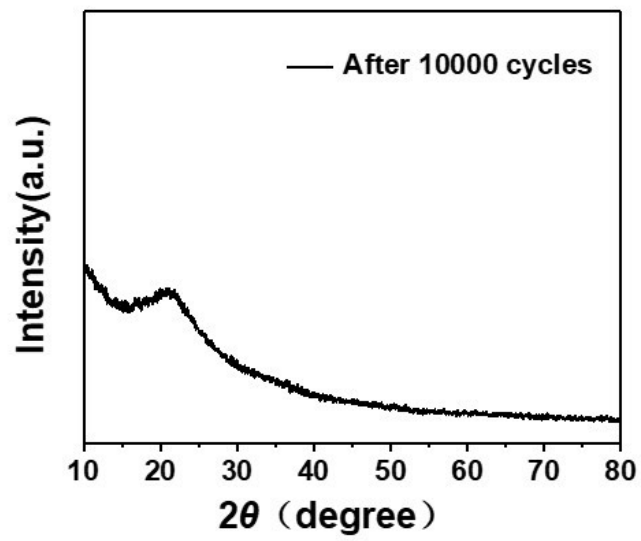


Fig. S17 The XRD pattern of the Fe-ISAs/H-CN after the 10000 cycles.

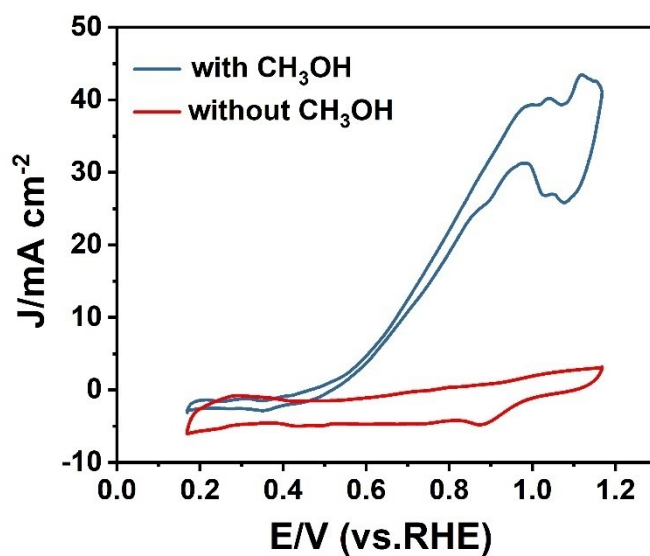


Fig. S18 The tolerance to methanol crossover test of the commercial Pt/C. CV curves of the 20 wt% Pt/C are measured in O₂-saturated 0.1 M KOH with and without 1.0 M CH₃OH at a scan rate of 50 mV s⁻¹.

Table S2 Comparison of the ORR activity between Fe-ISAs/H-CN and other catalysts under basic condition (0.1 M KOH) in literature.

Catalysts	$E_{1/2}$ (V vs.RHE)	Limited current (mA/cm ²)	Ref.
Fe-ISAs/p-CN	0.87	6.3	This work
Fe/OES	0.85	6.3	<i>Angew. Chem. Int. Ed.</i> 2020 , 59, 7384
Co-ISAS/p-CN	0.838	5.0	<i>Adv. Mater.</i> 2018 , 30, 1706508
Fe-N-C HNSs	0.87	5.9	<i>Adv. Mater.</i> 2019 , 31, 1806312
Fe-N/C-800	0.81	5.2	<i>J. Am. Chem. Soc.</i> 2015 , 137, 5555
FePhen@MOFArNH ₃	0.86	5.9	<i>Nat. Commun.</i> 2015 , 6, 7343
Fe/N/C-SCN	0.836	5.9	<i>Angew. Chem. Int. Ed.</i> 2015 , 54, 9907-9910
N-doped C/CNTs	0.82	5.5	<i>Angew. Chem. Int. Ed.</i> 2014 , 53, 4102-4106
Cu-N-C-60	0.8	5.5	<i>Energy Environ. Sci.</i> 2016 , 9, 3736-3745